gether with the values of the parameters $\xi kT/V_0$, κ and ζ that characterize networks A and B, respectively (see text), one may evaluate χ by solution of eq A-5. Results are given in Table II.

Equation A-10 in conjunction with A-7 may be solved iteratively for v_2', given the network parameters, the value of χ, and the extension ratio α_e relative to the system swollen to equilibrium under isotropic conditions. The reduced force that would obtain if further swelling did not occur as a result of the elongation α_e may be calculated according to eq 5 and eq I-54 of the preceding paper, with V/V_0 therein equated to $1/v_2$ and with $\lambda_\parallel$ and $\lambda_\perp$ determined by α_e and V/V_0 according to eq I-23. Repetition of the calculation with $V'/V_0 = 1/v_2'$, α_e' given by eq A-8, $\lambda_\perp$ given by eq A-7, and $\lambda_\parallel$ the same as above, yields the calculated reduced stress for the semiopen system at fixed length. The difference between the latter calculation and the former one gives the correction that should be subtracted from the observed reduced stress. Results shown in Figure 3 were corrected in this manner.

References and Notes

(1) Kuhn, W.; Grün, F. *Kolloid. Z.* **1942**, *101*, 248.
(2) Treloar, L. R. G. "The Physics of Rubber Elasticity", 3rd ed.; Clarendon Press: Oxford, 1975.
(3) Ong, C. S.; Stein, R. S. *J. Polym. Sci., Polym. Phys. Ed.* **1974**, *12*, 1599.
(4) Stein, R. S.; Farris, R. J.; Kumar, S.; Soni, V. *ACS Symp. Ser.* **1982**, *No. 193*, 453.
(5) Erman, B.; Flory, P. J. *Macromolecules*, preceding paper in this issue.
(6) Flory, P. J. *J. Chem. Phys.* **1977**, *66*, 5720.
(7) Flory, P. J.; Erman, B. *Macromolecules* **1982**, *15*, 800.
(8) Erman, B.; Flory, P. J. *Macromolecules* **1982**, *15*, 806.
(9) Benoit, H.; Stockmayer, W. H. *J. Phys. Radium* **1956**, *17*, 21.
(10) Prins, J. A.; Prins, W. *Physica (Amsterdam)* **1957**, *23*, 253.
(11) Kielich, S. *Acta Phys. Polonica* **1960**, *19*, 149; *J. Chem. Phys.* **1967**, *46*, 4090.
(12) Coumou, D. J.; Hijmans, J.; Mackor, E. L. *Trans. Faraday Soc.* **1964**, *60*, 2244. Coumou, D. J. *Ibid.* **1969**, *65*, 2654.
(13) Patterson, G. D.; Flory, P. J. *J. Chem. Soc., Faraday Trans. 2* **1972**, *68*, 1098.
(14) Gent, A. N.; Vickroy, V. V. *J. Polym. Sci., Polym. Phys. Ed.* **1967**, *5*, 47.
(15) Gent, A. N. *Macromolecules* **1969**, *2*, 262.
(16) Ishikawa, T.; Nagai, K. *J. Polym. Sci., Polym. Phys. Ed.* **1969**, *7*, 1123. *Polymer J.* **1970**, *1*, 116.
(17) Gent, A. N.; Kuan, T. H. *J. Polym. Sci., Polym. Phys. Ed.* **1971**, *9*, 927.
(18) Fukuda, M.; Wilkes, G. L.; Stein, R. S. *J. Polym. Sci., Polym. Phys. Ed.* **1971**, *9*, 1417.
(19) Rehage, G.; Schäfer, E. E.; Schwarz, J. *Angew. Makromol. Chem.* **1971**, *16/17*, 231.
(20) Liberman, M. H.; Abe, Y.; Flory, P. J. *Macromolecules* **1972**, *5*, 550.
(21) Liberman, M. H.; DeBolt, L. C.; Flory, P. J. *J. Polym. Sci., Polym. Phys. Ed.* **1974**, *12*, 187.
(22) Flory, P. J. *Faraday Discuss. Chem. Soc.* **1979**, *68*, 14.
(23) Shih, H.; Flory, P. J. *Macromolecules* **1972**, *5*, 758.
(24) Erman, B.; Marvin, D. C.; Irvine, P. A.; Flory, P. J. *Macromolecules* **1982**, *15*, 664.
(25) Ronca, G.; Allegra, G. *J. Chem. Phys.* **1975**, *63*, 4990.
(26) Flory, P. J. *Proc. R. Soc. London, Ser. A* **1976**, *351*, 351.
(27) Flory, P. J. *Polymer* **1979**, *20*, 1317.
(28) Birefringence measurements on unswollen sample B at higher extensions, i.e., for $\alpha_e^{-1} < 0.48$, were subject to errors due to extraneous effects of scattering of the beam from the boundaries of the sample. This was a consequence of the small width of the specimen under these conditions.
(29) Fischer, E. W.; Strobl, G. R.; Dettenmaier, M.; Stamm, M.; Steidl, N. *Faraday Discuss. Chem. Soc.* **1979**, *68*, 26.
(30) Le Fèvre, R. J. W. *Rev.* Pure *Appl. Chem.* **1970**, *20*, 67.
(31) Ingwall, R. T.; Czurylo, E. A.; Flory, P. J. *Biopolymers* **1973**, *12*, 1137.
(32) One of the two conformations of tetraethylmethane (TEM) may be viewed as the fusion of two *n*-pentane chains at their central atoms when both chains are trans,trans. This conformation is asymmetric in shape, being oblate ellipsoidal in form, but its polarizability tensor should be isotropic. The other eligible conformation formed from this one by gauche rotations of opposite signs about two of the central bonds possesses tetrahedral symmetry and therefore is roughly spherical. Its polarizability also should be isotropic.
(33) In the approximation of tetrahedral symmetry about Si and C, the tensor for the anisotropic part of the polarizability of the structural unit $O\text{–}Si(CH_3)_2\text{–}O$ is

$$\hat{\alpha} = \Delta\alpha \text{ diag } (\tfrac{2}{3}, 0, -\tfrac{2}{3})$$

where $\Delta\alpha$ is defined by eq 13 and the principal axes in the order of the diagonal elements are taken parallel to O···O, perpendicular thereto in the plane defined by the Si–O bonds, and parallel to $CH_3\cdots CH_3$, respectively. The anisotropy tensor for the PDMS chain as a whole in any conformation is a linear combination of the group tensors so defined, additivity of these tensors for individual units being assumed.
(34) Flory, P. J.; Rehner, J., Jr. *J. Chem. Phys.* **1943**, *11*, 521. Flory, P. J. *Trans. Faraday Soc.* **1961**, *57*, 829. Flory, P. J.; Tatara, Y. *J. Polym. Sci., Polym. Phys. Ed.* **1975**, *13*, 683.

More on the Model Parameters of Helical Wormlike Chains

Motoharu Fujii, Kyosuke Nagasaka, Jiro Shimada, and Hiromi Yamakawa*

Department of Polymer Chemistry, Kyoto University, Kyoto, Japan.
Received January 11, 1983

ABSTRACT: The model parameters of the helical wormlike chains corresponding to various real polymer chains, both flexible and stiff, are determined from a comparison with the rotational isomeric state models or from an analysis of experimental data for equilibrium and transport properties. Then some general aspects of the behavior of the model parameters are discussed. This serves to guess their probable ranges for a given new polymer. The results are useful in a study of the chain dynamics recently initiated on the basis of the discrete helical wormlike chain.

I. Introduction

In recent years, we have shown that the helical wormlike (HW) chain[1-3] can mimic the equilibrium conformational behavior of real chains as well as the rotational isomeric state (RIS) model.[4] However, the RIS model or conventional bond chains are not necessarily convenient for the treatment of steady-state transport and dynamic properties of real chains, both flexible and stiff. Thus, we have evaluated the steady-state transport coefficients on the basis of the HW cylinder model.[5,6] Further, we have recently started a study of the dynamics of dilute polymer solutions on the basis of the discrete HW chain[7-9] whose equilibrium conformational behavior is almost identical with that of the (continuous) HW chain. In order to proceed to make an extensive analysis of, for instance, local motions of various real chains, as probed from dielectric

0024-9297/83/2216-1613$01.50/0

relaxation, nuclear magnetic relaxation, and fluorescence depolarization, along this line, the model parameters of the corresponding continuous HW chains must be determined. In fact, for some polymers, this has already been done from a comparison with the RIS model or from an analysis of experimental data for equilibrium and transport properties.[1,2,5,6] Thus, the object of the present paper is to do this for other important and interesting polymers.

The plan of the present paper is as follows. In section II, we give a short sketch of the model. In section III, we summarize fundamental quantities to be analyzed. In section IV, we analyze experimental data for symmetric chains. In sections V–VII, we analyze the RIS data for monosubstituted and disubstituted asymmetric chains and polymers of other types, respectively. In section VIII, the model parameters thus determined are summarized, and some general aspects of their behavior are discussed. This serves to guess their probable ranges for a given new polymer.

II. Short Sketch of the Model

The HW chain is defined as an elastic wire model[1,2] with both bending and torsional energies such that when its total configurational energy becomes a minimum of zero, its contour takes a helical form. This regular helix (as a space curve) is specified by the constant curvature κ_0 and torsion τ_0 and is referred to as the characteristic helix. The chain stiffness is represented by the stiffness parameter λ^{-1}, which has the dimension of length and is proportional to the bending force constant, the ratio of the bending and torsional force constants being equal to $1 + \sigma$, with σ the Poisson ratio. Note that values to be assigned the σ defined on the microscopic level are not necessarily equal to those ($\sigma \simeq 0.5$) for bulk polymers. As a consequence, we can affix the localized Cartesian coordinate system [$\mathbf{e}_\xi(s)$, $\mathbf{e}_\eta(s)$, $\mathbf{e}_\zeta(s)$] to the chain at the contour point s with the ξ, η, and ζ axes defined as follows.[10] The ζ axis is taken along the tangent vector of the chain contour, and the ξ and η axes coincide with the principal axes of inertia for the cross section at s. Further, the $\mathbf{e}_\xi$ agrees with the unit mean curvature vector of the chain contour. When we want to adapt the HW chain to a given real chain on the monomer unit level, it is necessary to assign properly a localized coordinate system to a certain rigid body part in the monomer unit of the latter corresponding to that of the former. In any case, we must convert the total contour length L of the former to the number of bonds in the latter or the molecular weight M. This is done by introducing the shift factor M_L, as defined as the molecular weight per unit contour length of the continuous model. Thus, the basic parameters of the HW chain are κ_0, τ_0, λ^{-1}, σ, and M_L.

III. Fundamental Quantities To Be Analyzed

In this section, we briefly summarize quantities to be analyzed. The first three subsections deal with the angular correlation functions,[11] the persistence vector,[12,13] the characteristic ratio, and the mean-square radius of gyration. These quantities except the mean-square radius of gyration are not experimentally observable, but all are useful for a comparison of the HW chain with the RIS model. Some other experimentally observable quantities are considered in the last subsection.

Angular Correlation Functions. Consider the HW chain of total contour length L and its subchain separated by two arbitrary contour points t_1 and t_2 with the contour distance $t = t_2 - t_1$ ($0 \le t_1 \le t_2 \le L$) between them. In what follows, we assume that $\sigma = 0$, as in most of the cases studied previously, since the results are rather insensitive to variation in σ,[2] and measure all lengths of the HW chain, as usual, in units of the stiffness parameter λ^{-1} unless noted otherwise. Its statistical mechanical properties may be determined by the Green's function $G(\Omega|\Omega_0;t)$ of $\Omega(t_2) = \Omega$ when $\Omega(t_1) = \Omega_0$, where $\Omega = (\theta,\phi,\psi)$ denotes the Euler angles defining the orientation of the localized Cartesian coordinate system ($\mathbf{e}_\xi,\mathbf{e}_\eta,\mathbf{e}_\zeta$) affixed to the chain with respect to an external coordinate system. It may be expanded in the form[10,14]

$$G(\Omega|\Omega_0;t) = \sum_{l,m,j,j'} g_l^{jj'}(t)\mathcal{D}_l^{mj}(\Omega)\mathcal{D}_l^{mj'*}(\Omega_0) \quad (1)$$

where $\mathcal{D}_l^{mj}$ is the normalized Wigner function defined by eq 15-17 of SMHWC-II,[14] the asterisk indicating the complex conjugate. The sums over $\mathcal{D}_l^{mj}$ are taken over $l \ge 0$, $|m| \le l$, and $|j| \le l$ unless specified otherwise. The expansion coefficients $g_l^{jj'}(t)$, which are dependent on t_1 and t_2 as $t = t_2 - t_1$, may be written as eq 2 of SMHWC-VIII[11]

$$g_l^{jj'}(t) = 8\pi^2\langle \mathcal{D}_l^{mj*}(\Omega)\mathcal{D}_l^{mj'}(\Omega_0)\rangle \quad (2)$$

where the angular brackets indicate the average over Ω and Ω_0, so that $g_l^{jj'}(t)$ have the meaning of the angular correlation functions. They are the fundamental quantities in the statistical mechanics of the HW chain. In fact, all kinds of equilibrium moments may be expressed in terms of them. In the present case of $\sigma = 0$, $g_l^{jj'}(t)$ are given by eq 10 with eq 7 and 8 of ref 7 or eq A1 with eq A4–A8 and A17–A20 of SMHWC-X.[15] For later use, it is convenient to give the explicit expressions for the real parts $\bar{g}_1^{jj'}$ of the four independent components of $g_1^{jj'}$, i.e., g_1^{00}, $g_1^{0(-1)}$, $g_1^{1(-1)}$, and $g_1^{(-1)(-1)}$

$$\bar{g}_1^{00}(t) = \nu^{-2}e^{-2t}[\kappa_0^2 \cos(\nu t) + \tau_0^2]$$

$$\bar{g}_1^{0(-1)}(t) = 2^{-1/2}\kappa_0\nu^{-1}e^{-2t}\sin(\nu t)$$

$$\bar{g}_1^{1(-1)}(t) = \tfrac{1}{2}\kappa_0^2\nu^{-2}e^{-2t}[1 - \cos(\nu t)]$$

$$\bar{g}_1^{(-1)(-1)}(t) = \tfrac{1}{2}\nu^{-2}e^{-2t}[\kappa_0^2 + (\kappa_0^2 + 2\tau_0^2)\cos(\nu t)] \quad (3)$$

with

$$\nu = (\kappa_0^2 + \tau_0^2)^{1/2} \quad (4)$$

Next, we consider a conventional bond chain or the RIS model. We can affix a localized Cartesian coordinate system to a certain rigid body part (e.g., composed of two adjacent skeletal bonds) in the monomer unit (see sections IV–VI). Let $\Omega_0 = (\theta_0,\phi_0,\psi_0)$ and $\Omega = (\theta,\phi,\psi)$ be the orientations of the localized coordinate systems affixed to the pth and $q(=p + x)$th monomer units, respectively, with respect to the external coordinate system. If we assume that $p \gg 1$ and $N - q \gg 1$, with N the number of monomer units in the chain, we may ignore the end effect to define the Green's function $G(\Omega|\Omega_0;x)$. Then, the similar angular correlation functions $g_l^{jj'}(x)$ between two monomer units separated by x monomer units along the chain may be defined. $g_l^{jj'}(x)$ may be written in the same form as the $g_l^{jj'}(t)$ in eq 2 and are dependent on p and q as $x = q - p$. These $g_l^{jj'}(x)$ depend on the relative orientation $\hat{\Omega}$ of the localized system affixed to the monomer unit with respect to that monomer unit. We must determine $\hat{\Omega}$ from a comparison of the HW chain with the bond chain. However, it is, to some extent, restricted to preserve certain symmetry properties of $g_l^{jj'}(t)$ for the HW chain in $g_l^{jj'}(x)$ for the bond chain.[11]

Now, $g_l^{jj'}$ for the two models may be equated, and therefore we have

$$g_l^{jj'}(t) = g_l^{jj'}(x) \quad (5)$$

t is related to x by

$$\log t = \log x - \delta \quad (6)$$

with

$$\delta = \log (M_L/\lambda M_0) \tag{7}$$

where M_0 is the molecular weight of the monomer unit. Thus, from best fits of the HW values of $g_l^{jj'}$ plotted against log t to the RIS values plotted against log x, we may determine κ_0, τ_0, δ, and $\tilde{\Omega}$. Since $g_l^{jj'}$ is a dimensionless quantity, λ^{-1} and M_L cannot be determined separately from eq 7.

Finally, we note that the extent to which the relative orientation $\tilde{\Omega}$ is restricted depends, in general, on the physical quantity to be considered. The restriction is most severe for the angular correlation functions, and it may be somewhat relaxed for the persistence vector. $\tilde{\Omega}$ need not be considered for the mean-square end-to-end distance and mean-square radius of gyration without any restrictions.

Persistence Vectors. The persistence vector **A** of the HW chain is defined as the average of the end-to-end vector **R** with the orientation Ω_0 of the initial localized coordinate system ($\mathbf{e}_{\xi_0}$, $\mathbf{e}_{\eta_0}$, $\mathbf{e}_{\zeta_0}$) fixed[13]; i.e.

$$\mathbf{A} = \langle \mathbf{R} \rangle_{\Omega_0} \tag{8}$$

In the remainder of this subsection, we omit the subscript 0 referring to the initial localized system. The ξ, η, and ζ components of **A** in that system are given by eq 3 with eq 4 of SMHWC-IV[13] with $t = L$ and $\sigma = 0$, which may be rewritten as

$$\langle \xi \rangle = \kappa_0(4 + \nu^2)^{-1} - \kappa_0\nu^{-1}(4 + \nu^2)^{-1}e^{-2L}[\nu \cos(\nu L) + 2 \sin(\nu L)]$$

$$\langle \eta \rangle = \tfrac{1}{2}\kappa_0\tau_0(4 + \nu^2)^{-1} - \kappa_0\tau_0\nu^{-2}e^{-2L}\{\tfrac{1}{2} - (4 + \nu^2)^{-1}[2 \cos(\nu L) - \nu \sin(\nu L)]\}$$

$$\langle \zeta \rangle = \tfrac{1}{2}c_\infty - \nu^{-2}e^{-2L}\{\tfrac{1}{2}\tau_0^2 + \kappa_0^2(4 + \nu^2)^{-1}[2 \cos(\nu L) - \nu \sin(\nu L)]\} \tag{9}$$

with

$$c_\infty = (4 + \tau_0^2)/(4 + \kappa_0^2 + \tau_0^2) \tag{10}$$

Flory[12] has defined the persistence vector **A** of the RIS model as the mean end-to-end vector with the first and second bonds fixed and used a molecular Cartesian coordinate system ($\mathbf{e}_x$,$\mathbf{e}_y$,$\mathbf{e}_z$) such that the x axis is taken along the first bond, the y axis is in the plane of the first and second bonds, and the z axis completes the right-handed system. (Note that the molecular coordinate system ($\mathbf{e}_x$,$\mathbf{e}_y$,$\mathbf{e}_z$) defined for amylose in section VII is different from that defined above.) We designate the components of **A** (RIS) in this system by $\langle x \rangle$, $\langle y \rangle$, and $\langle z \rangle$.

We wish to equate the **A** for the two models. Suppose that the (initial) HW localized coordinate system ($\mathbf{e}_\xi$,$\mathbf{e}_\eta$,$\mathbf{e}_\zeta$) is obtained by rotation of the (initial) RIS molecular coordinate system ($\mathbf{e}_x$,$\mathbf{e}_y$,$\mathbf{e}_z$) through the Euler angles $\tilde{\Omega} = (\tilde{\theta},\tilde{\phi},\tilde{\psi})$. If $\mathbf{A}(\xi,\eta,\zeta)$ and $\mathbf{A}(x,y,z)$ are the column forms of **A** of the HW chain in the two systems, we have

$$\mathbf{A}(\xi,\eta,\zeta) = \mathbf{Q}(\tilde{\theta},\tilde{\phi},\tilde{\psi})\cdot\mathbf{A}(x,y,z) \tag{11}$$

with **Q** the rotational transformation matrix. Thus, the components of $\mathbf{A}(x,y,z)$ calculated from the inverse of eq 11 by assigning proper values to $\tilde{\Omega}$ may be equated to $\langle x \rangle$, $\langle y \rangle$, and $\langle z \rangle$.

Following the procedure of SMHWC-IV,[13] we analyze the HW and RIS values. The parameters to be determined are κ_0, τ_0, λ^{-1}, M_L, and $\tilde{\Omega}$. Let $\mathbf{A}_\infty$ be **A** for an infinitely long chain. We first equate $A_\infty = |\mathbf{A}_\infty|$ of the HW chain to that of the RIS model

$$\lambda^{-1}A_\infty(\mathrm{HW}) = A_\infty(\mathrm{RIS}) \tag{12}$$

where the **A** of the RIS model has not been reduced by λ^{-1}. (Recall that all lengths of the HW chain are reduced by λ^{-1}.) If κ_0 and τ_0 are given, A_∞(HW) may be computed from eq 9, and therefore λ^{-1} may be determined from eq 12 with the value of A_∞(RIS). With these values of κ_0, τ_0, λ^{-1}, and A_∞, $\tilde{\Omega}$ may then be determined to give the coincidence between the directions of $\mathbf{A}_\infty$ of the two models and also a best fit of the values of the components of $\lambda^{-1}\mathbf{A}(x,y,z)$ of the HW chain as a function of L to the values of $\langle x \rangle$, $\langle y \rangle$, and $\langle z \rangle$ of the RIS model. Starting with various sets of κ_0 and τ_0, we repeat this procedure until a final best fit is found. Finally, M_L may be determined from the factor δ in the relation

$$\log L = \log x - \delta \tag{13}$$

where δ is given by eq 7 and x is the total number of monomer units in the RIS model (not to be confused with the Cartesian coordinate x). The factor δ may be determined from a best fit of the values of $\lambda^{-1}A$(HW) as a function of L to those of A(RIS) as a function of x (where $A = |\mathbf{A}|$).

We note that theoretically $\tilde{\Omega}$ is uniquely related to $\hat{\Omega}$ introduced in the last subsection, but this relation is not necessarily satisfied exactly with their values determined as above.

Characteristic Ratios and Mean-Square Radii of Gyration. The mean-square end-to-end distance $\langle R^2 \rangle$ and mean-square radius of gyration $\langle S^2 \rangle$ of the HW chain of total contour length L are given by eq 54 and 56 of SMHWC-I[2] with $t = L$ and $\sigma = 0$, respectively, which may be rewritten in the forms

$$\langle R^2 \rangle = c_\infty L - \tfrac{1}{2}\tau_0^2\nu^{-2} - 2\kappa_0^2\nu^{-2}(4 - \nu^2)(4 + \nu^2)^{-2} + e^{-2L}\{\tfrac{1}{2}\tau_0^2\nu^{-2} + 2\kappa_0^2\nu^{-2}(4 + \nu^2)^{-2}[(4 - \nu^2)\cos(\nu L) - 4\nu \sin(\nu L)]\} \tag{14}$$

$$\langle S^2 \rangle = \tau_0^2\nu^{-2}\langle S^2 \rangle_{\mathrm{KP}} + \kappa_0^2\nu^{-2}\left[\frac{L}{3r}\cos\gamma - \frac{1}{r^2}\cos(2\gamma) + \frac{2}{r^3L}\cos(3\gamma) - \frac{2}{r^4L^2}\cos(4\gamma) + \frac{2}{r^4L^2}e^{-2L}\cos(\nu L + 4\gamma)\right] \tag{15}$$

with

$$r = (4 + \nu^2)^{1/2} \tag{16}$$

$$\gamma = \cos^{-1}(2/r) \tag{17}$$

Here, ν and c_∞ are given by eq 4 and 10, respectively, and $\langle S^2 \rangle_{\mathrm{KP}}$ is the $\langle S^2 \rangle$ of the Kratky–Porod (KP) wormlike chain[16] with the same λ^{-1} as that of the HW chain under consideration and is given by

$$\langle S^2 \rangle_{\mathrm{KP}} = \frac{L}{6} - \frac{1}{4} + \frac{1}{4L} - \frac{1}{8L^2}(1 - e^{-2L}) \tag{18}$$

Note that the KP chain is a special case of the HW chain with $\kappa_0 = 0$ and that eq 18 has been derived originally by Benoit and Doty.[17]

Let l be the bond length in the RIS model and reduce all lengths except l by λ^{-1}, so that $\langle R^2 \rangle$ and $\langle S^2 \rangle$ of the RIS model are also reduced. Recalling that $\langle R^2 \rangle$(RIS) = $\lambda^2 C_n n l^2$, we set $\langle R^2 \rangle$(RIS) equal to $\langle R^2 \rangle$(HW), where C_n is the characteristic ratio for the RIS chain of n bonds. Therefore, we have

$$\langle R^2 \rangle/\langle R^2 \rangle_{(\mathrm{C})}(\mathrm{HW}) = C_n/C_\infty \qquad (=\langle R^2 \rangle/\langle R^2 \rangle_{(\mathrm{C})}(\mathrm{RIS})) \tag{19}$$

where $\langle R^2 \rangle_{(\mathrm{C})}$ are the coil limiting values of $\langle R^2 \rangle$ and are given by

$$\langle R^2 \rangle_{(\mathrm{C})} = c_\infty L \qquad (\mathrm{HW}) \tag{20}$$

$$\langle R^2\rangle_{(C)} = \lambda^2 C_\infty n l^2 \qquad \text{(RIS)} \tag{21}$$

with C_∞ the characteristic ratio at $n = \infty$. L is related to the total number x of monomer units by eq 13. The parameters κ_0, τ_0, and δ may be determined from a best fit of the values of $\langle R^2\rangle/\langle R^2\rangle_{(C)}$(HW) as a function of L to those of C_n/C_∞ as a function of x. Equating the two $\langle R^2\rangle_{(C)}$ given by eq 20 and 21 with $L = \lambda x M_0/M_L$ and $n = n_0 x$, we also have the relation

$$\lambda^{-1} = C_\infty n_0 M_L l^2/c_\infty M_0 \tag{22}$$

where n_0 is the number of bonds in the monomer unit. Thus, we may determine λ^{-1} and M_L from eq 7 and 22. The analysis of $\langle S^2\rangle$ is almost the same as above if $\langle R^2\rangle$ is replaced by $\langle S^2\rangle$ in eq 19, and the relation $\langle S^2\rangle_{(C)} = \langle R^2\rangle_{(C)}/6$ is used.

Some Other Experimentally Observable Quantities. In this paper, we consider only the mean-square dipole moments and the temperature coefficients of $\langle R^2\rangle_{(C)}$, and not other observable quantities such as electric birefringence and dichroism,[15] optical anisotropy,[43] and steady-state transport coefficients,[5,6,33] which may be used to determine the model parameters.

Consider the HW chain of total contour length L and let $\mathbf{m}(s)$ be the local electric dipole moment vector per unit length at the contour point s, expressed in the localized Cartesian coordinate system. (We assume that $\mathbf{m}(s)$ is independent of s.) Its mean-square dipole moment $\langle\mu^2\rangle$ is given by eq 18 of SMHWC-X;[15] i.e.

$$\langle\mu^2\rangle = m^2\langle\hat{R}^2\rangle \tag{23}$$

with $m = |\mathbf{m}|$. $\langle\hat{R}^2\rangle$ is the mean-square end-to-end distance of the HW chain of total contour length L such that the constant curvature and torsion of its characteristic helix are equal to $\hat{\kappa}_0$ and $\hat{\tau}_0$, respectively, and it is given by eq 14 with $\kappa_0 = \hat{\kappa}_0$ and $\tau_0 = \hat{\tau}_0$, where $\hat{\kappa}_0$ and $\hat{\tau}_0$ are given by

$$\hat{\kappa}_0 = (\nu^2 - \hat{\tau}_0^2)^{1/2} \tag{24}$$

$$\hat{\tau}_0 = (\kappa_0 m_\eta + \tau_0 m_\zeta)/m \tag{25}$$

with

$$\nu = (\kappa_0^2 + \tau_0^2)^{1/2} = (\hat{\kappa}_0^2 + \hat{\tau}_0^2)^{1/2} \tag{26}$$

and $\mathbf{m} = (m_\xi, m_\eta, m_\zeta)$ in the localized coordinate system $(\mathbf{e}_\xi, \mathbf{e}_\eta, \mathbf{e}_\zeta)$.

An analysis of $\langle\mu^2\rangle$ may be made as follows. We consider double-logarithmic plots of $\langle\mu^2\rangle/x$ against x by use of the equation

$$\log(\langle\mu^2\rangle/x) = \log(\langle\hat{R}^2\rangle/\hat{c}_\infty L) + \log(m^2\hat{c}_\infty M_0/\lambda M_L) \tag{27}$$

with eq 13, where $\hat{c}_\infty$ is given by eq 10 with $\hat{\kappa}_0$ and $\hat{\tau}_0$ in place of κ_0 and τ_0, respectively, m being unreduced. The parameters $\hat{\kappa}_0$ and $\hat{\tau}_0$ and the ratios $M_L/\lambda M_0$ and $m^2\hat{c}_\infty M_0/\lambda M_L$ may be determined from a best fit of double-logarithmic plots of the theoretical $\langle\hat{R}^2\rangle/\hat{c}_\infty L$ against L to double-logarithmic plots of observed $\langle\mu^2\rangle/x$ against x. However, it should be noted that a determination of the individual parameters requires some assumptions. (See section IV.)

Next, for the HW chain, if we assume that the unreduced κ_0, τ_0, and L are independent of temperature and that λ^{-1} is proportional to T^{-1}, with T the absolute temperature, we have[3]

$$\frac{d\ln\langle R^2\rangle_{(C)}}{dT} = -\frac{16 - 4\kappa_0^2 + (8 + \kappa_0^2 + \tau_0^2)\tau_0^2}{(4 + \tau_0^2)(4 + \kappa_0^2 + \tau_0^2)}T^{-1} \tag{28}$$

where $\langle R^2\rangle_{(C)}$ is unreduced. Thus, κ_0 and τ_0 cannot be determined separately from the observed temperature coefficient alone. However, it is useful in conjunction with some of the quantities mentioned above.

IV. Symmetric Chains

We have already determined the model parameters for polymethylene (PM), poly(oxymethylene) (POM), and poly(dimethylsiloxane) (PDMS), which fall under the category of symmetric chains.[1,11,13,15] In this section, we make an analysis of experimental data for $\langle\mu^2\rangle$, C_∞, and the temperature coefficient of the latter for poly(oxyethylene) (POE), although the RIS values are available. Note that POE also falls under this category but differs from the above polymers in the sense that its monomer unit is composed of three skeletal bonds.

Poly(oxyethylene). For convenience, we take as a rigid body part in the monomer unit of POE the one composed of the successive C–O and O–C bonds. It is known that the preferred conformation of POE is ttg^+ or ttg^- for the bond sequence C–O–C–C,[4] where t, g^+, and g^- denote the trans, gauche$^+$, and gauche$^-$ states, respectively. For this bond chain, the ζ axis is taken along a line passing through the two C of C–O–C, the ξ axis is in the plane of the C→O and O→C bonds with its positive direction chosen at an acute angle with the C→O bond, and the η axis completes the right-handed system. Then, the real parts of $g_l^{jj'}$ for POE in this system have the same symmetry properties as those for the corresponding HW chain, irrespective of the value of τ_0.[11] (If $\tau_0 = 0$, the symmetry properties of $g_l^{jj'}$ for both chains completely agree with each other.) If the permanent dipole moment of POE is assumed to arise from the O–C (and C–O) bonds, it follows that its local moment $\mathbf{m}$ is in the direction of $\mathbf{e}_\xi$, so that it has perpendicular (type B) dipoles with $m = m_\xi$ ($m_\eta = m_\zeta = 0$). Then we also have $\hat{\kappa}_0 = \nu$ and $\hat{\tau}_0 = 0$ from eq 24 and 25.

Experimental data for $\langle\mu^2\rangle$ are available for two series of POE homologues, one having hydroxyl terminal groups, $HO(CH_2CH_2O)_xOH$,[18-20] and the other having ethyl terminal groups, $C_2H_5O(CH_2CH_2O)_{x-1}C_2H_5$.[19,21] The former series have the large bond dipole moments $m_{HO} = 1.7$ D at the chain ends, which are appreciably larger than the intermediate bond dipole moments $m_{CO} = 0.99$ D.[4] Therefore, we analyze the data only for the latter series for small x, at which the end effects are appreciable. We adopt the data for the latter series at 20 °C[19] and at 25 °C[21] and also the data for the former series with $x \gtrsim 80$ at 20 °C[20] and at 25 °C,[19] all data having been obtained in benzene. Figure 1 shows double-logarithmic plots of $\langle\mu^2\rangle/x$ against x with these data, $\langle\mu^2\rangle$ being expressed in D^2 (where we have ignored the temperature difference). The ratio decreases with increasing x (for $x \geq 3$), and the POE chain may be regarded as a typical HW chain. The curve in the figure represents the best fit theoretical values calculated from eq 27 with $\hat{\kappa}_0 = 2.5$, $\hat{\tau}_0 = 0$, $\log(M_L/\lambda M_0) = 0.38$, and $\log(m^2\hat{c}_\infty M_0/\lambda M_L) = 0.06$. Recall that a determination of the individual parameters requires some assumptions.

If we set $\tau_0 = 0$, as required by the symmetry properties of the symmetric (POE) chain,[11] then we have $\hat{\kappa}_0 = \kappa_0 = 2.5$ and $\hat{\tau}_0 = \tau_0 = 0$ (25 °C) from eq 24–26. With these values of κ_0 and τ_0, we have $d\ln\langle R^2\rangle_{(C)}/dT = 0.66 \times 10^{-3}$ deg^{-1} (at 60 °C) from eq 28. However, this value of the temperature coefficient is larger than the observed value 0.23×10^{-3} deg^{-1} (at 60 °C).[22] Therefore, we ignore the restriction $\tau_0 = 0$ and determine κ_0 and τ_0 from $\nu = 2.5$ ($=\hat{\kappa}_0$) and eq 28 with the observed value of the temperature coefficient. Then, we find $\kappa_0 = 2.4$ and $\tau_0 = 0.5$. Finally, we obtain $\lambda^{-1} = 12.0$ Å and $M_L = 8.8$ Å^{-1} from eq 22 with $\log(M_L/\lambda M_0) = 0.38$ and the observed $C_\infty = 4.0$ (at 40

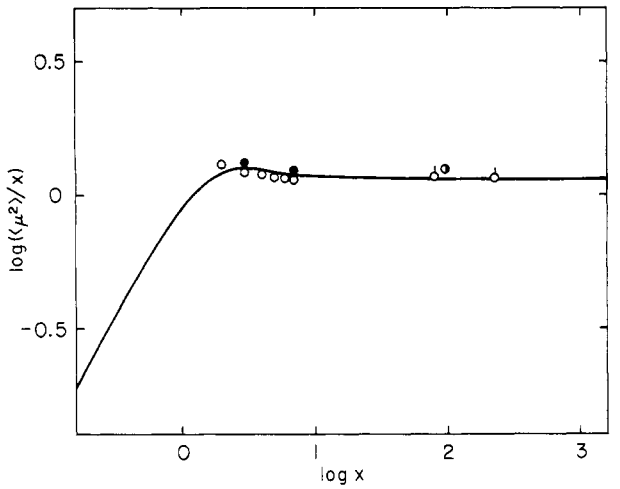

Figure 1. Analysis of the data for $\langle\mu^2\rangle$ according to eq 27 with eq 13 for poly(oxyethylene) homologues $C_2H_5O(CH_2CH_2O)_{x-1}C_2H_5$ in benzene at 25 °C (○)[21] and at 20 °C (●)[19] and for homologues $HO(CH_2CH_2O)_xOH$ in benzene at 25 °C (◇)[19] and at 20 °C (◑).[20] The curve represents the best fit theoretical values.

°C),[22] and then m = 0.22 D/Å from log $(m^2\hat{c}_\infty M_0/\lambda M_L)$ = 0.06 with these values of λ^{-1} and M_L (n_0 = 3, M_0 = 44, and the root-mean-square bond length l = 1.46 Å).

V. Monosubstituted Asymmetric Chains

We have already determined the model parameters for isotactic and syndiotactic polypropylenes (i- and s-PP)[1] and isotactic and syndiotactic polystyrenes (i- and s-PS).[11,13] In this section, we analyze the RIS values of the angular correlation functions, the persistence vector, the characteristic ratio, and the mean-square radius of gyration for some other monosubstituted asymmetric chains following the procedure of section III.

For convenience, we take as a rigid body part in the monomer unit of the asymmetric chain the one composed of the successive C–C$^\alpha$ and C$^\alpha$–C bonds. As in SMHWC-VIII,[11] our localized system $(\mathbf{e}_{\xi_x},\mathbf{e}_{\eta_x},\mathbf{e}_{\zeta_x})$ affixed to the xth monomer unit composed of the $(k-1)$th and kth skeletal bonds corresponding to the system $(\mathbf{e}_\xi,\mathbf{e}_\eta,\mathbf{e}_\zeta)$ of the HW chain is taken as follows. $\mathbf{e}_{\zeta_x}$ is parallel to $\mathbf{l}_{k-1}+\mathbf{l}_k$, with $\mathbf{l}_k$ the kth bond vector, and $\mathbf{e}_{\xi_x}$ is obtained by rotation of $\mathbf{e}'$ through an angle $\hat{\psi}$ about the ζ_x axis, where $\mathbf{e}'$ is a unit vector in the plane of $\mathbf{l}_{k-1}$ and $\mathbf{l}_k$ with $\mathbf{e}'\cdot\mathbf{e}_{\zeta_x}=0$, with its positive direction chosen at an acute angle with $\mathbf{l}_{k-1}$. $\hat{\Omega}$ is then uniquely related to $\hat{\psi}$. The angle $\hat{\psi}$ is a parameter to be determined by a comparison of the RIS model with the HW chain. We take the C–C$^\alpha$ and C$^\alpha$–C bonds as the first and second bonds, respectively, in the sequence to be considered and assume that first bond to be d-chiral, where we have adopted the new Flory convention[23] to describe the stereochemical configuration of the asymmetric chain. (This choice corresponds to case i for the asymmetric chain mentioned in SMHWC-VIII.)

The parameters required for the computation of the RIS values[23] are the bond length l_{C-C^α} (=1.53 Å), the two supplementary bond angles θ' and θ'' at the CH_2 and C$^\alpha$, respectively, the rotation angles ϕ about the bond in the trans (t), gauche (g), and gauche (ḡ) states,[23] and the energy parameters η, τ, ω, ω', and ω''. For the RIS model, $\mathbf{A}$, C_n, and $\langle S^2\rangle$ are computed by the matrix generation technique,[4,12,24] and $g_1^{jj'}$ following the procedure of SMHWC-VIII.[11] All numerical work has been done with the use of a FACOM M-382 digital computer in this university.

Poly(methyl acrylate). The values of the RIS model parameters adopted for isotactic and syndiotactic poly(methyl acrylate) (i- and s-PMA) chains[25] are the following:

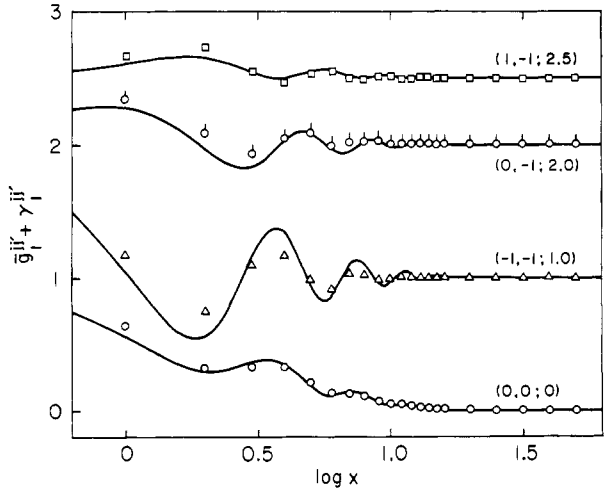

Figure 2. $\bar{g}_1^{jj'}+\gamma_1^{jj'}$ plotted against log x for isotactic PMA chains, where x is the number of monomer units. The points represent the RIS values, and the curves the HW values; the attached numbers in the parentheses indicate the values of $(j,j';\gamma_1^{jj'})$.

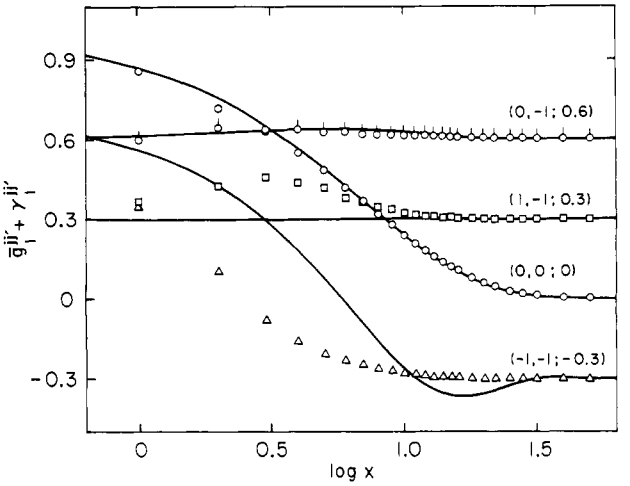

Figure 3. $\bar{g}_1^{jj'}+\gamma_1^{jj'}$ plotted against log x for syndiotactic PMA chains; see legend to Figure 2.

θ' = 66° and θ'' = 68°; ϕ = 10° (t) and 110° (g) (ḡ being inhibited); and η = 1.60, ω = 0.00235, ω' = 0.0268, and ω'' = 0.126 at 300 K.

The values of $\bar{g}_1^{jj'}+\gamma_1^{jj'}$, with $\gamma_1^{jj'}$ being appropriate constants, are plotted against log x in Figures 2 and 3 for i- and s-PMA chains, respectively, where the numbers in the parentheses attached to the curves indicate the values of $(j,j';\gamma_1^{jj'})$. The open circles, circles with pips, squares, and triangles represent the RIS values for $\bar{g}_1^{00}$, $\bar{g}_1^{0(-1)}$, $\bar{g}_1^{1(-1)}$, and $\bar{g}_1^{(-1)(-1)}$, respectively, with $\hat{\psi}=3\pi/2$ for i-PMA and $\hat{\psi}=0$ for s-PMA. The values assigned to $\hat{\psi}$ are $3\pi/2$ and 0 for all isotactic and syndiotactic chains studied in this section, respectively. The curves in these figures represent the best fit HW values calculated from eq 3 with κ_0 = 6.5, $|\tau_0|$ = 11, and δ = 0.89 for i-PMA and κ_0 = 0.35, $|\tau_0|$ = 2.0, and δ = 1.15 for s-PMA. The behavior of $\bar{g}_1^{jj'}$ for i- and s-PMA is quite similar to that for i- and s-PS displayed in SMHWC-VIII, respectively. For i-PMA, $\bar{g}_1^{jj'}$ for the two models agree well with each other. On the other hand, for s-PMA, this is also the case except for $\bar{g}_1^{(-1)(-1)}$. Since we cannot determine λ^{-1} and M_L separately from the analysis of $\bar{g}_1^{jj'}$, we determine them from eq 7 and 22 with n_0 = 2, M_0 = 86, the values of κ_0 and τ_0, and the RIS values of C_∞ (=8.22 for i-PMA and 19.1 for s-PMA). Thus, we have λ^{-1} = 20.0 Å and M_L = 33.4 Å^{-1} for i-PMA and λ^{-1} = 35.8 Å and M_L = 33.9 Å^{-1} for s-PMA.

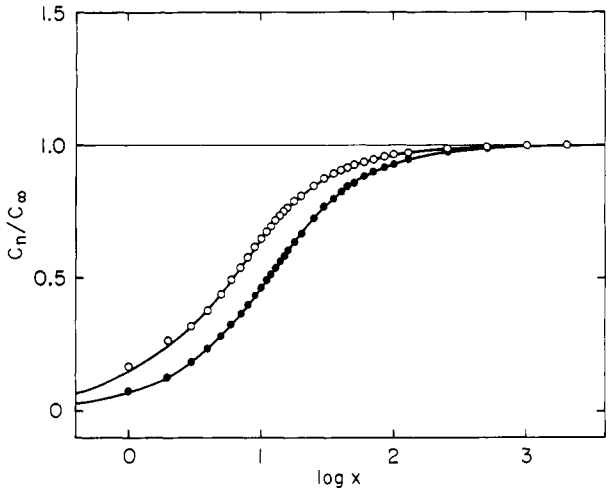

Figure 4. Characteristic ratio C_n/C_∞, relative to C_∞, plotted against log x for PMA chains, where x is the number of monomer units. The open and filled circles represent the RIS values for the isotactic and syndiotactic chains, respectively. The curves represent the HW values.

Next, we analyze the persistence vector **A**. Its behavior for i- and s-PMA is also similar to that for i- and s-PS, respectively. (See Figures 4 and 5 of SMHWC-IV[13] or Figures 3 and 4 of ref 26.) The components of $\mathbf{A}_\infty$ are found to be $\langle x\rangle_\infty$ = 5.09 Å, $\langle y\rangle_\infty$ = 7.66 Å, and $\langle z\rangle_\infty$ = 1.46 Å for i-PMA and $\langle x\rangle_\infty$ = 15.8 Å, $\langle y\rangle_\infty$ = 9.37 Å, and $\langle z\rangle_\infty$ = 2.73 Å for s-PMA. If we use the values of κ_0 and τ_0 determined from $\bar{g}_1^{jj'}$ as their first trial values, we find that the agreement between the RIS and HW values of the components of **A** is satisfactory. With these values of κ_0 and τ_0, we obtain λ^{-1} = 21.5 Å and M_L = 31.6 Å^{-1} for i-PMA and λ^{-1} = 37.5 Å and M_L = 33.1 Å^{-1} for s-PMA. We note that the orientations of the initial HW localized coordinate systems with respect to the initial Flory molecular coordinate systems ($\mathbf{e}_x$,$\mathbf{e}_y$,$\mathbf{e}_z$) are $\tilde{\Omega}$ = (105.7°,39.0°,−136.4°) and $\tilde{\Omega}$ = (88.5°,29.4°,125.1°) for i- and s-PMA, respectively. We note that the persistence vector for s-PMA exhibits many small oscillations, but the model parameters above have been determined neglecting these oscillations. This is also the case with other syndiotactic chains studied in this section.

Finally, we analyze C_n and $\langle S^2\rangle$. The characteristic ratios C_n/C_∞, relative to C_∞, are plotted against log x in Figure 4. The open and filled circles represent the RIS values for i- and s-PMA, respectively. As seen from Figure 4, C_n increase monotonically with increasing x for i- and s-PMA. In such a case, we cannot determine κ_0 and τ_0 accurately from an analysis of C_n. Therefore, we use the values of κ_0 and τ_0 determined from the analysis of $\bar{g}_1^{jj'}$. The curves in the figure represent the HW values calculated from eq 14 with κ_0 = 6.5, $|\tau_0|$ = 11, and δ = 0.90 for i-PMA and κ_0 = 0.35, $|\tau_0|$ = 2.0, and δ = 1.16 for s-PMA. From eq 7 and 22, we then find λ^{-1} = 20.2 Å and M_L = 33.7 Å^{-1} for i-PMA and λ^{-1} = 36.1 Å and M_L = 34.3 Å^{-1} for s-PMA. If we analyze $\langle S^2\rangle$ in a similar way, we have λ^{-1} = 19.1 Å and M_L = 31.8 Å^{-1} for i-PMA and λ^{-1} = 35.3 Å and M_L = 33.5 Å^{-1} for s-PMA.

As shown above, the consistency in the values of the model parameters determined from the various quantities is satisfactory. This is also the case with the other polymers studied in this section. The values of the model parameters determined above fall in the ranges λ^{-1} = 19.1–21.5 Å and M_L = 31.6–33.7 Å^{-1} for i-PMA and λ^{-1} = 35.3–37.5 Å and M_L = 33.1–34.3 Å^{-1} for s-PMA. Thus, we adopt as the values of κ_0, τ_0, λ^{-1}, and M_L those determined from $\bar{g}_1^{jj'}$ in conjunction with C_∞, for convenience. Finally, we note that the general behavior of all the quantities under consideration for i- and s-PMA is similar to that for the other isotactic and syndiotactic chains studied in this section, respectively. In the following, therefore, we do not repeat the details of the analysis and results.

Poly(methyl vinyl ketone). The values of the RIS model parameters adopted for isotactic and syndiotactic poly(methyl vinyl ketone) (i- and s-PMVK) chains[27] are the following: θ' = 66° and θ'' = 68°; ϕ = 10° (t) and 110° (g) ($\bar{g}$ being inhibited); and η = 2.5, ω = 0.05, ω' = 0.02, and ω'' = 0.008 at 300 K. From an analysis of $\bar{g}_1^{jj'}$ with C_∞, we find κ_0 = 22, $|\tau_0|$ = 33, δ = 1.35, λ^{-1} = 53.2 Å, and M_L = 29.5 Å^{-1} (C_∞ = 18.7) for i-PMVK and κ_0 = 0.1, $|\tau_0|$ = 2.0, δ = 1.41, λ^{-1} = 65.1 Å, and M_L = 27.6 Å^{-1} (C_∞ = 35.2) for s-PMVK. The values of the parameters determined from the various quantities fall in the ranges λ^{-1} = 49.5–53.2 Å and M_L = 27.5–29.5 Å^{-1} for i-PMVK and λ^{-1} = 65.0–67.0 Å and M_L = 26.8–27.6 Å^{-1} for s-PMVK.

Poly(vinyl acetate). The values of the RIS model parameters adopted for isotactic and syndiotactic poly(vinyl acetate) (i- and s-PVAc) chains[28] are the following: θ' = 66° and θ'' = 70.5°; and η = 1.94, τ = 0.174, ω = 0.151, ω' = 0.183, and ω'' = 0.145 at 300 K. The rotation angles are rather complicated: for the meso dyad, (ϕ,ϕ') = (21°,21°) for tt, (105°,3°) for gt, (−104°,10°) for $\bar{g}$t, (96°,84°) for gg, (91°,−108°) for g$\bar{g}$, and (−102°,−102°) for $\bar{g}\bar{g}$; for the racemic dyad, (ϕ,ϕ') = (8°,8°) for tt, (96°,8°) for gt, (−113°,10°) for $\bar{g}$t, (104°,104°) for gg, (72°,−108°) for g$\bar{g}$, and (−98°,−98°) for $\bar{g}\bar{g}$, where ϕ and ϕ' are the rotation angles about the C$^\alpha$→C and C→C$^\alpha$ bonds in the dyad C$^\alpha$CC$^\alpha$, respectively. From an analysis of $\bar{g}_1^{jj'}$ with C_∞, we find κ_0 = 4.0, $|\tau_0|$ = 8.6, δ = 0.78, λ^{-1} = 15.1 Å, and M_L = 34.4 Å^{-1} (C_∞ = 6.7) for i-PVAc and κ_0 = 0.4, $|\tau_0|$ = 2.5, δ = 1.23, λ^{-1} = 42.0 Å, and M_L = 34.7 Å^{-1} (C_∞ = 21.9) for s-PVAc. The values of the parameters determined from the various quantities fall in the ranges λ^{-1} = 13.7–17.5 Å and M_L = 28.8–34.4 Å^{-1} for i-PVAc and λ^{-1} = 41.5–43.4 Å and M_L = 33.6–34.7 Å^{-1} for s-PVAc.

Poly(vinyl chloride). The values of the RIS model parameters adopted for isotactic and syndiotactic poly(vinyl chloride) (i- and s-PVC) chains[29] are the following: θ' = θ'' = 68°; ϕ = 0° (t), 120° (g), and −120° ($\bar{g}$); and η = 4.2, τ = 0.45, ω = 0.032, ω' = 0.071, and ω'' = 0.032 at 298 K. The characteristic ratios C_n as functions of x were computed by Mark.[29] However, we have also calculated C_n since its values at large x are not available. From an analysis of $\bar{g}_1^{jj'}$ with C_∞, we find κ_0 = 6.0, $|\tau_0|$ = 16.5, δ = 0.93, λ^{-1} = 20.4 Å, and M_L = 26.1 Å^{-1} (C_∞ = 9.2) for i-PVC and κ_0 = 0.14, $|\tau_0|$ = 2.0, δ = 1.49, λ^{-1} = 78.0 Å, and M_L = 24.8 Å^{-1} (C_∞ = 42.0) for s-PVC. The values of the parameters determined from the various quantities fall in the ranges λ^{-1} = 19.4–21.3 Å and M_L = 24.9–26.1 Å^{-1} for i-PVC and λ^{-1} = 77.1–79.6 Å and M_L = 23.6–24.8 Å^{-1} for s-PVC.

Poly(vinyl bromide). The values of the RIS model parameters adopted for isotactic and syndiotactic poly(vinyl bromide) (i- and s-PVB) chains[30] are the following: θ' = 66° and θ'' = 68°; ϕ = 0° (t), 120° (g), and −120° ($\bar{g}$); and η = 1.28, τ = 0.438, ω = 0.0162, ω' = 0.0369, and ω'' = 0.00263 at 303 K. We note that C_∞ = 14.3 for the isotactic chain is larger than C_∞ = 11.3 for the syndiotactic chain. This is not the case with the other polymers studied in this section. From an analysis of $\bar{g}_1^{jj'}$ with C_∞, we find κ_0 = 17, $|\tau_0|$ = 25, δ = 1.16, λ^{-1} = 37.6 Å, and M_L = 41.1 Å^{-1} for i-PVB and κ_0 = 0.7, $|\tau_0|$ = 1.9, δ = 0.97, λ^{-1} = 22.9 Å, and M_L = 43.5 Å^{-1} for s-PVB. The values of the parameters determined from the various quantities fall in the ranges λ^{-1} = 36.2–38.1 Å and M_L = 39.7–41.1 Å^{-1} for i-PVB and λ^{-1} = 22.1–23.5 Å and M_L = 41.4–43.5 Å^{-1} for s-PVB.

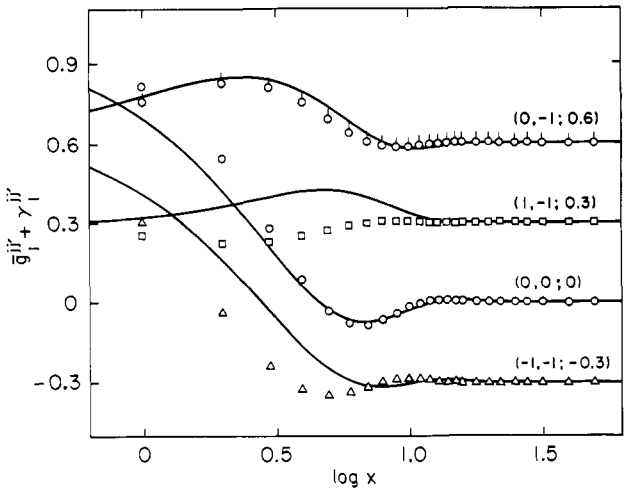

Figure 5. $\bar{g}_1^{jj'} + \gamma_1^{jj'}$ plotted against log x for isotactic PαMS chains; see legend to Figure 2.

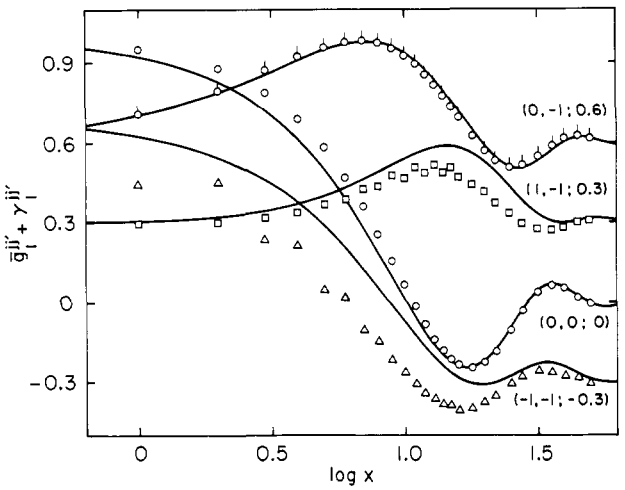

Figure 6. $\bar{g}_1^{jj'} + \gamma_1^{jj'}$ plotted against log x for syndiotactic PαMS chains; see legend to Figure 2.

VI. Disubstituted Asymmetric Chains

We have already determined the model parameters for isotactic and syndiotactic poly(methyl methacrylate)s (i- and s-PMMA).[2,11,13] In this section, we analyze the RIS values of the angular correlation functions, the persistence vector, the characteristic ratio, and the mean-square radius of gyration for isotactic and syndiotactic poly(α-methylstyrene) (i- and s-PαMS) chains following the procedure of section III. The localized system ($\mathbf{e}_{\xi_x}$,$\mathbf{e}_{\eta_x}$,$\mathbf{e}_{\zeta_x}$) of the RIS model may be affixed to the monomer unit in the same fashion as for the monosubstituted asymmetric chains described in section V.

Poly(α-methylstyrene). The values of the RIS model parameters adopted for i- and s-PαMS chains[31] are the following: $\theta' = 58°$ and $\theta'' = 70.5°$; for the meso dyad, $(\phi,\phi') = (7°,7°)$ for tt, (105°,14°) for gt, and (120°,120°) for gg; for the racemic dyad, $(\phi,\phi') = (14°,14°)$ for tt, (105°,14°) for gt, and (120°,120°) for gg ($\bar{g}$ being inhibited); and the energy parameters are taken as $\alpha = 0.435$ and $\beta = 5.29$ at 300 K.

Figures 5 and 6 show plots of $\bar{g}_1^{jj'} + \gamma_1^{jj'}$ against log x for i- and s-PαMS, respectively, where $\hat{\psi} = \pi$ for both i- and s-PαMS. The symbols in the figures have the same meaning as in Figures 2 and 3. The curves in these figures represent the best fit HW values calculated from eq 3 with $\kappa_0 = 2.3$, $|\tau_0| = 1.0$, and $\delta = 0.81$ for i-PαMS and $\kappa_0 = 4.4$, $|\tau_0| = 1.0$, and $\delta = 1.45$ for s-PαMS. The behavior of $\bar{g}_1^{jj'}$ for i- and s-PαMS is quite similar to that for i- and s-PMMA displayed in SMHWC-VIII,[11] respectively. There is good agreement between the RIS and HW values except for $\bar{g}_1^{(-1)(-1)}$. From eq 7 and 22 with $n_0 = 2$, $M_0 = 118$, these values of κ_0 and τ_0, and the RIS values of C_∞ (=5.12 for i-PαMS and 9.09 for s-PαMS), we find $\lambda^{-1} = 17.8$ Å and $M_L = 42.7$ Å^{-1} for i-PαMS and $\lambda^{-1} = 76.5$ Å and $M_L = 43.5$ Å^{-1} for s-PαMS.

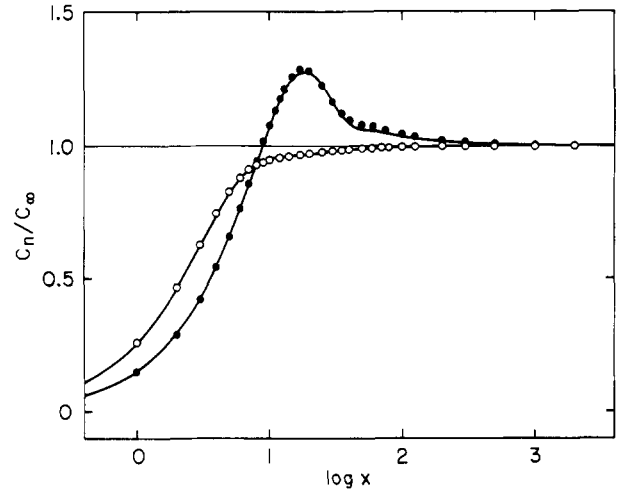

Figure 7. Characteristic ratio C_n/C_∞, relative to C_∞, plotted against log x for PαMS chains; see legend to Figure 4.

Next we analyze the persistence vector **A**. Its behavior for i- and s-PαMS is also similar to that for i- and s-PMMA, respectively. (See Figures 6 and 7 of SMHWC-IV[13] or Figures 5 and 6 of ref 26.) The components of $\mathbf{A}_\infty$ are found to be $\langle x\rangle_\infty = 3.06$ Å, $\langle y\rangle_\infty = 6.00$ Å, and $\langle z\rangle_\infty = 2.58$ Å for i-PαMS and $\langle x\rangle_\infty = 1.30$ Å, $\langle y\rangle_\infty = 15.8$ Å, and $\langle z\rangle_\infty = -3.43$ Å for s-PαMS. If we use the values of κ_0 and τ_0 determined from $\bar{g}_1^{jj'}$ as their first trial values, we find that the agreement between the RIS and HW values of the components of **A** is rather good. However, for s-PαMS, the agreement is further improved with slightly different values of κ_0 and τ_0. In this case, we have $\kappa_0 = 4.0$, $\tau_0 = 0$, $\lambda^{-1} = 71.6$ Å, and $M_L = 39.5$ Å^{-1} for s-PαMS.

Finally, we analyze C_n and $\langle S^2\rangle$. The characteristic ratios C_n/C_∞, relative to C_∞, are plotted against log x in Figure 7. The open and filled circles represent the RIS values for i- and s-PαMS, respectively. The characteristic ratio of s-PαMS as a function of x exhibits a maximum. (Figure 7 is to be compared with Figure 3 of SMHWC-I.[2]) The curves in the figure represent the best fit HW values calculated from eq 14 with $\kappa_0 = 2.3$, $|\tau_0| = 1.0$, and $\delta = 0.86$ for i-PαMS and $\kappa_0 = 4.1$, $|\tau_0| = 1.0$, and $\delta = 1.45$ for s-PαMS. From eq 7 and 22, we then find $\lambda^{-1} = 18.9$ Å and $M_L = 45.2$ Å^{-1} for i-PαMS and $\lambda^{-1} = 72.3$ Å and $M_L = 45.9$ Å^{-1} for s-PαMS. If we analyze $\langle S^2\rangle$ in a similar way, we have $\kappa_0 = 2.3$, $|\tau_0| = 1.0$, $\lambda^{-1} = 15.9$ Å, and $M_L = 38.0$ Å^{-1} for i-PαMS and $\kappa_0 = 3.8$, $|\tau_0| = 0.6$, $\lambda^{-1} = 66.3$ Å, and $M_L = 42.6$ Å^{-1} for s-PαMS. Note that for i-PαMS, these values of κ_0 and τ_0 are the same as those determined from $\bar{g}_1^{jj'}$ and also **A**.

As shown above, the consistency in the values of the model parameters determined from the various quantities is satisfactory. They fall in the ranges $\lambda^{-1} = 15.9$–20.7 Å and $M_L = 38.0$–45.2 Å^{-1} for i-PαMS and $\kappa_0 = 3.8$–4.4, $|\tau_0| = 0$–1.0, $\lambda^{-1} = 66.3$–76.5 Å, and $M_L = 39.5$–43.5 Å^{-1} for s-PαMS. Thus, we adopt as the values of κ_0, τ_0, λ^{-1}, and M_L those determined from $\bar{g}_1^{jj'}$ in conjunction with C_∞, for convenience.

VII. Other Polymers

We have already determined the model parameters for poly(DL-alanine) (PDLA),[32] poly(n-butyl isocyanate)

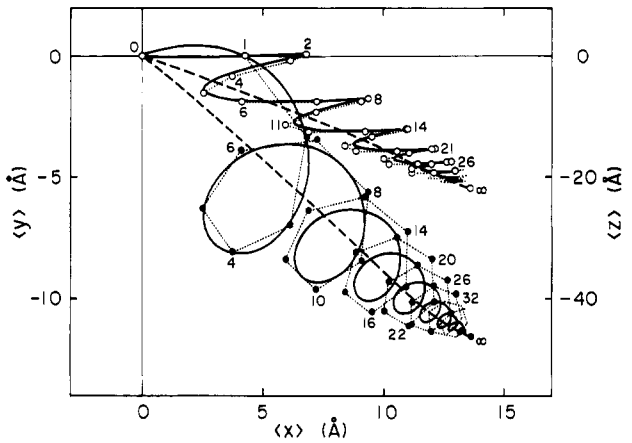

Figure 8. Components $\langle y \rangle$ and $\langle z \rangle$ of the persistence vector **A** plotted against the component $\langle x \rangle$ for amylose. The filled and open circles represent the values of $\langle y \rangle$(RIS) and $\langle z \rangle$(RIS),[34] respectively, the attached numbers indicating the values of x, the number of virtual bonds. The full and broken curves represent the HW values in cases 1 and 2, respectively. The dotted lines connecting the circles trace the progression of increasing x.

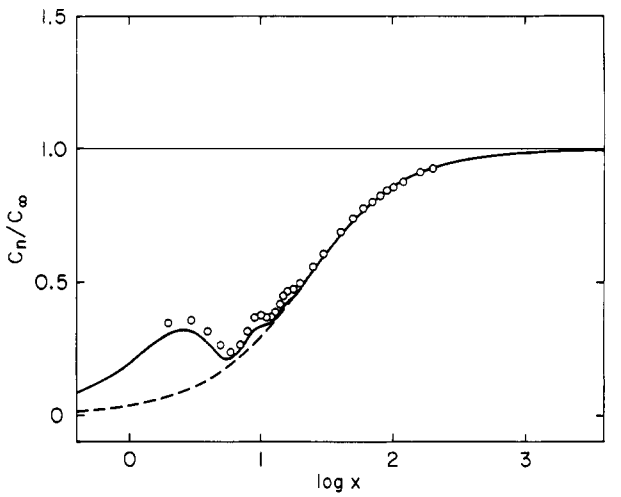

Figure 9. Characteristic ratio C_n/C_∞, relative to C_∞, plotted against log x for amylose, where x is the number of virtual bonds. The points represent the RIS values.[34] The full and broken curves represent the HW values in cases 1 and 2, respectively.

(PBIC),[15] DNA,[9] and some other stiff-chain polymers.[33] In this section, we analyze the RIS values for those polymers that may be regarded as chains of virtual bonds.

Amylose. Jordan et al.[34] calculated the persistence vector **A** and the characteristic ratio C_n ($\equiv\langle R^2\rangle/xl^2$) as a function of the number x of virtual bonds of length l (=4.25 Å) for amylose in aqueous solution at 25 °C. The molecular Cartesian coordinate system ($\mathbf{e}_x$,$\mathbf{e}_y$,$\mathbf{e}_z$) is affixed to the first glucose residue as follows:[35] the x axis is taken along the first virtual bond, which connects successive glycosidic oxygens, the y axis is in the plane of that virtual bond and the $O_4 \rightarrow C_4$ bond in the first glucose residue with its positive direction chosen at an acute angle with that $O_4 \rightarrow C_4$ bond, and the z axis completes the right-handed Cartesian coordinate system. In Figure 8 the components $\langle y \rangle$ and $\langle z \rangle$ of **A** are plotted against the component $\langle x \rangle$. The filled and open circles represent the values of $\langle y \rangle$(RIS) and $\langle z \rangle$(RIS), respectively, the attached numbers indicating the values of x. These values have been taken from Figures 11 of ref 34. The components of $\mathbf{A}_\infty$ are $\langle x \rangle_\infty$ = 13.6 Å, $\langle y \rangle_\infty$ = −11.6 Å, and $\langle z \rangle_\infty$ = −21.8 Å. The dotted lines connecting the circles trace the progression of increasing x. In a comparison with the HW chain, we consider the following two cases: case 1, the contour of the HW chain is taken along the actual helical sequence; case 2, the chain contour is taken along the helix axis, assuming the larger length scales. The full curves represent the best fit HW values in case 1 calculated from eq 9 and 11 with κ_0 = 28, τ_0 = 12, δ = 1.465, λ^{-1} = 141 Å, M_L = 33.4 Å^{-1} (M_0 = 162), and $\tilde{\Omega}$ = (99.1°,23.3°,−118.9°). The broken curves represent the best fit HW values in case 2 with κ_0 = 0.2, τ_0 = 2.0, δ = 1.46, λ^{-1} = 56.5 Å, M_L = 82.7 Å^{-1}, and $\tilde{\Omega}$ = (136.7°,−39.4°,−54.2°).

Next we analyze the characteristic ratio. Figure 9 shows plots of the characteristic ratio C_n/C_∞, relative to C_∞, against log x. The open circles represent the values of C_n/C_∞ of Jordan et al.,[34] where C_∞ has been found to be 4.8 by an extrapolation of C_n to x^{-1} = 0. The full and broken curves represent the HW values calculated from eq 14 with δ = 1.46 in case 1 and δ = 1.44 in case 2, respectively, and with the values of κ_0 and τ_0 determined from the persistence vector in each case. From eq 7 and 22, we then find λ^{-1} = 125 Å and M_L = 37.3 Å^{-1} in case 1 and λ^{-1} = 48.9 Å and M_L = 91.3 Å^{-1} in case 2. As seen from Figure 9, for both the RIS model and the HW chain in case 1, C_n exhibits oscillations in the range $x \lesssim 30$ and then increases monotonically to C_∞ as x is increased. In this connection, we note that case 2 is to be adopted in an analysis of the steady-state transport coefficients as discussed in ref 33 and also that $\langle S^2\rangle/M$ in dimethyl sulfoxide has been observed to decrease with increasing molecular weight M,[36-39] showing the typical HW behavior.[1,2]

Polycarbonate of Diphenylol-2,2′-propane. The spatial configuration of the polycarbonate of diphenylol-2,2′-propane (PC) chain may be expressed in terms of virtual bonds that extend from the quaternary C to the intersection (X) of the extensions of the C^{ph}–O bonds.[40-42] In order to adapt the HW chain to the PC chain, the localized coordinate system ($\mathbf{e}_\xi$,$\mathbf{e}_\eta$,$\mathbf{e}_\zeta$) of the latter corresponding to that of the former *should* be affixed to the (monomer) unit composed of two adjacent virtual bonds in such a way that $\mathbf{e}_\zeta$ is in the direction of the sum of the two adjacent virtual bond vectors. Then, the HW chain can mimic the PC chain only on the relatively large length scales, so that we consider only the characteristic ratio.

The rotation about each virtual bond is considered to be subject to a twofold symmetric potential. Therefore, the PC chain obeys freely rotating chain statistics as far as the characteristic ratio is concerned. The values of the RIS model parameters adopted are the following:[42] virtual bond length l = 6.86 Å and supplementary bond angles θ_1 (at the quaternary C) = 70.5° and θ_2 (at the X) = 46°. The characteristic ratio C_n ($\equiv\langle R^2\rangle/xl^2$) for this (freely rotating) chain composed of x virtual bonds (X→quaternary C) (with x even) is given by

$$C_n = \frac{(1+\cos\theta_1)(1+\cos\theta_2)}{1-\cos\theta_1\cos\theta_2} - \frac{2\cos\theta_2(1+\cos\theta_1)^2}{x(1-\cos\theta_1\cos\theta_2)^2}[1-(\cos\theta_1\cos\theta_2)^{x/2}] \quad (29)$$

Thus, the PC chain may be represented by the HW chain with $\kappa_0 = \tau_0 = 0$ (i.e., the KP2 chain[43]) on the length scales mentioned above, and we find δ = 0.46, λ^{-1} = 20.0 Å, and M_L = 18.3 Å^{-1} from an analysis of C_n (C_∞ = 2.94) (n_0 = 1 and M_0 = 127).

Poly(2,6-dimethyl-1,4-phenylene oxide). For a poly(2,6-dimethyl-1,4-phenylene oxide) (M_2PPO) chain, the situation is similar to that of the PC chain. Its spatial configuration may be expressed in terms of virtual bonds that connect successive ether oxygens.[41,44] The M_2PPO chain also obeys freely rotating chain statistics. The values

Table I
Values of the Model Parameters for Various Polymer Chains

polymer	temp, K	κ_0	$\lvert\tau_0\rvert$	λ^{-1}, Å	M_L, Å^{-1}
Symmetric Chains					
PM	413	0.3[a]	0[a]	14.5[a]	10.1[a]
PDMS	298	2.6[b]	0[b]	20.7[b]	19.6[b]
POM	303	17[a]	25[a]	22.3	13.1
POE	298	2.4[c]	0.5[c]	12.0[c]	8.8[c]
Monosubstituted Asymmetric Chains					
i-PP	413	3.7	5.0	11.9	16.1
s-PP	413	0.6	2.4	23.9	16.8
i-PS	300	11[a]	15[a]	26.4[a]	41.2[a]
s-PS	300	0.8[a]	2.3[a]	37.5	41.9
i-PMA	300	6.5	11	20.0	33.4
s-PMA	300	0.35	2.0	35.8	33.9
i-PMVK	300	22	33	53.2	29.5
s-PMVK	300	0.1	2.0	65.1	27.6
i-PVAc	300	4.0	8.6	15.1	34.4
s-PVAc	300	0.4	2.5	42.0	34.7
i-PVC	298	6.0	16.5	20.4	26.1
s-PVC	298	0.14	2.0	78.0	24.8
i-PVB	303	17	25	37.6	41.1
s-PVB	303	0.7	1.9	22.9	43.5
Disubstituted Asymmetric Chains					
i-PMMA	300	1.7[a]	1.4[a]	32.7[a]	33.5[a]
s-PMMA	300	4.4[a]	0.8[a]	65.6[a]	35.7[a]
i-PαMS	300	2.3	1.0	17.8	42.7
s-PαMS	300	4.4	1.0	76.5	43.5
Other Polymers					
PDLA	300	6.5[d]	0[d]	28.3[d]	14.7[d]
PC	298	0	0	20.0	18.3
M_2PPO	300	0	0	14.8	20.4
amylose	298	28[e]	12[e]	141[e]	33.4[e]
	298	0.2[f]	2.0[f]	56.5[f]	82.7[f]
	298	4.9[g]	1.0[g]	630[g]	79[g]
PBIC	296	0[h]	1890	1440[h]	55.1[h]
DNA	293	0[i]	200[i]	1100[i]	195

[a] See ref 11. [b] From experimental data; see ref 15. [c] From experimental data; see the text. [d] See ref 32. [e] From RIS data in aqueous solution in case 1; see the text. [f] From RIS data in aqueous solution in case 2; see the text. [g] From experimental data in dimethyl sulfoxide; see ref 33. [h] From experimental data; see ref 15. [i] See ref 9.

of the RIS model parameters adopted are the following:[41] virtual bond length l = 5.50 Å and supplementary bond angles $\theta_1 = \theta_2$ (at the ether oxygens) = 61°. Then, the characteristic ratio C_n ($\equiv\langle R^2\rangle/xl^2$) for the M_2PPO chain composed of x virtual bonds (with x even) is given by eq 29. It may also be regarded as the HW chain with $\kappa_0 = \tau_0 = 0$, and we find δ = 0.40, λ^{-1} = 14.8 Å, and M_L = 20.4 Å^{-1} from an analysis of C_n (C_∞ = 2.88) (n_0 = 1 and M_0 = 120).

VIII. Model Parameters

We have determined the HW model parameters from a comparison with the RIS model with respect to $\bar{g}_1^{jj'}$ with C_∞ (or **A**) in most cases and from an analysis of experimental data in some cases. In this section, all the results obtained thus far (here and previously) are summarized, and some general aspects of the behavior of the model parameters are discussed. In Table I are given the values of κ_0, τ_0, λ^{-1}, and M_L at the indicated temperatures. We may assume that the unreduced κ_0 and τ_0 are independent of temperature T and that λ^{-1} is proportional to T.[3] Recall that λ^{-1} is proportional to the bending force constant but is not equal to the Kuhn segment length A_K for $\kappa_0 \neq 0$, the latter being defined by

$$A_K = c_\infty \lambda^{-1} \tag{30}$$

where c_∞ is given by eq 10 (c_∞ = 1 for κ_0 = 0). (Therefore, $(2\lambda)^{-1}$ is not equal to the so-called persistence length for $\kappa_0 \neq 0$.) Recall also that the shift factor M_L is closely related to the length scales adopted for a given polymer (see below).[1]

First, we make some remarks on the results for POM, s-PS, and i- and s-PP given in Table I. The values of λ^{-1} for POM and s-PS were determined previously from $\bar{g}_1^{jj'}$ assuming the values of M_L determined from **A**.[11] However, the values of κ_0 and τ_0 from $\bar{g}_1^{jj'}$ are somewhat different from those determined from **A**, especially for s-PS, because of the difference in the length scale adopted in these analyses.[11] Therefore, the values of λ^{-1} and M_L redetermined here from $\bar{g}_1^{jj'}$ and C_∞ are listed in Table I. For i-PP and s-PP, the model parameters also have been redetermined from $\bar{g}_1^{jj'}$ and C_∞, since they were determined previously from **A**.[1] We note that the values of the temperature coefficient of the unperturbed chain dimension $\langle R^2\rangle_{(C)}$ for i-PP and s-PP in Table I of ref 3 remain unchanged with these new values of κ_0 and τ_0.

Next, some comments are required on the results for Other Polymers (except for PDLA) of Table I. First, we reconsider the adaptation of the HW chains to the PC and M_2PPO chains, for which we have chosen $\kappa_0 = \tau_0 = 0$. We have affixed the localized coordinate system to the rigid body part composed of two adjacent virtual bonds. However, in the real PC and M_2PPO chains, the chain conformation depends on the rotation of the phenylene group about the virtual bond, and this fact cannot be taken into account by the above adaptation. Therefore, on the basis of the discrete HW chain, we cannot study the local motions such as the rotation of the phenylene group about the virtual bond, as probed from nuclear magnetic relaxation. Thus, the HW chain can mimic these polymers only on the relatively large length scales. We also note that the KP chain[3] cannot explain the experimental fact that $\langle R^2\rangle_{(C)}$ of these polymers are independent of temperature.[45-48]

Second, the three sets of the model parameters are given for amylose. The first two are valid for amylose in aqueous solution,[34] and the difference between them arises from the length scales adopted, as mentioned in section VII. The third have been determined from an analysis of the sedimentation coefficient for amylose in dimethyl sulfoxide at 25 °C,[33] corresponding to the relatively large length scales. In this case, it is clearly seen that, in general, M_L is larger on the larger length scales for a given polymer.

Third, we must discuss the values of τ_0 for PBIC and DNA. It is well-known that DNA may be represented by the KP chain (with κ_0 = 0). However, we must also determine the value of τ_0 if we want to study, for instance, the cyclization and dynamic problems of DNA. In the case of DNA, this can be achieved if a localized Cartesian coordinate system is affixed to each base pair, representing it by the KP1 chain[43] with κ_0 = 0 and $\tau_0 \neq 0$. Since its one helix turn contains 10 base pairs, we then have $\tau_0 \simeq 200$,[9] assuming λ^{-1} = 1100 Å (in 0.2 M NaCl) and the distance between base pairs equal to 3.4 Å. Similarly, in the case of PBIC, if a localized system is affixed to its monomer unit, we have $\tau_0 \simeq 1890$, assuming λ^{-1} = 1440 Å and M_L = 55.1 Å^{-1}, as determined previously,[15] and the Troxell–Scheraga[49] and Shmueli–Traub–Rosenheck[50] 8_3 helices. We note that for the KP chain (κ_0 = 0), C_n, $\langle S^2\rangle$, $\langle\mu^2\rangle$ (for parallel dipole polymers), and the steady-state transport coefficients are independent of τ_0.

Now, it is convenient to plot the values of κ_0 and τ_0 in a (κ_0,τ_0) plane as in Figure 10, where the points with $\kappa_0 \leq$

Table II
Values of the Coefficients A_k (k = 2-7) as Functions of κ_0 and $|\tau_0|$ in Eq A4 of Ref 9

κ_0	$\lvert\tau_0\rvert$	A_2	A_3	A_4	A_5	A_6	A_7
6.5	11	−1.0337(−3)[a]	−2.1958(−1)	2.8242	5.7896	−2.9010(1)	3.2462(1)
4.0	8.6	−1.8954(−3)	−1.0864	1.4980 (1)	−5.2381(1)	7.6711(1)	−3.4028(1)

[a] $a(n)$ means $a \times 10^n$.

5 and $\tau_0 \leq 3$ are not shown in its insert. The polymers listed in Table I (except with $\kappa_0 = 0$) are identified by the numbers attached to the points (see the caption of Figure 10). The (κ_0,τ_0) plane is divided into three domains, I, II, and III, where the broken curve a is the boundary between the domains I and II and the chain curve b is the boundary between the domains II and III.[51] The ratio $\langle R^2\rangle/c_\infty L$ $(=C_n/C_\infty)$ as a function of L exhibits at least one maximum in the domains I and II, and the first peak (occurring as L is increased) is higher and lower than the coil limiting value of unity in I and II, respectively. In the domain III, the ratio is an increasing function of L but exhibits inflection in some cases. For example, s-PαMS, amylose in aqueous solution in case 1, and PMA lie in the domains I, II, and III, respectively (see Figures 4, 7, and 9). We note that the oscillations of $\bar{g}_1^{ij'}$ as functions of t become remarkable for large ν beyond the shaded domain ($10 \leq \nu \leq 15$) in the insert of Figure 10 and also that the HW chains with positive temperature coefficients of unperturbed chain dimensions belong to the domain I with $\tau_0 \lesssim 2$.[3]

It is seen that the points corresponding to the values of κ_0 and τ_0 for the asymmetric chains are rather systematically distributed in the (κ_0,τ_0) plane. The points for the isotactic monosubstituted asymmetric chains are nearly on a straight line passing through the origin. This is not difficult to understand, considering the fact that the preferred conformations for these chains are $(tg^+)_x$ and $(tg^-)_x$, leading to right- and left-handed 3_1 helices,[4] so that they have almost the same unreduced κ_0 and τ_0 (i.e., the ratio τ_0/κ_0 is constant). Recall that the reduced κ_0 and τ_0 are equal to the unreduced ones multiplied by λ^{-1}. Thus, polymers with larger ν at constant τ_0/κ_0 have larger λ^{-1}. We note that the larger λ^{-1}, the larger C_∞, as far as these polymers are concerned. The points for the syndiotactic monosubstituted asymmetric chains are in the neighborhood of the point with $\kappa_0 = 0.5$ and $\tau_0 = 2$. The points for the syndiotactic disubstituted asymmetric chains are in the domain I, indicating that these chains are the typical HW chains.[51] Their helical nature arises from the two different bond angles in conjunction with the predominance of trans,trans conformation for racemic dyads.[2,52] On the other hand, the points for the isotactic disubstituted asymmetric chains are located between those for syndiotactic monosubstituted and disubstituted asymmetric chains.

Finally, it is pertinent to note that the calculated values of the temperature coefficient are positive for PDMS, POE, s-PMMA, s-PαMS, PDLA, and amylose in dimethyl sulfoxide, and so are the observed values for the first three.[3]

IX. Concluding Remarks

In this paper, we have determined the model parameters of the HW chains corresponding to various real chains from an analysis of the RIS values or the experimental data and discussed some general aspects of their behavior, especially for monosubstituted and disubstituted asymmetric chains. Thus, we can guess the probable ranges of the model parameters for a given new polymer, especially as far as it belongs to this category.

Besides the polymers listed in Table I, we have already made an analysis of experimental data for $\langle S^2\rangle$ and the steady-state transport coefficients for cellulose acetate, poly(phthaloyl-*trans*-2,5-dimethylpiperazine), and poly(terephthaloyl-*trans*-2,5-dimethylpiperazine) on the basis of the HW chain[33] and found that the first two may be better represented by the HW chain, but the third by the KP chain. However, the model parameters thus determined for them cannot necessarily be used for the study of local chain motions associated with smaller length scales and therefore have not been included in Table I. (Note also that they are not very accurate.) Further, we know some polymers, such as poly(alkene sulfone) and poly(styrene oxide), whose local motions are gaining a great interest,[53-55] but we have not attempted to determine their model parameters because of the present lack of the detailed conformational information.

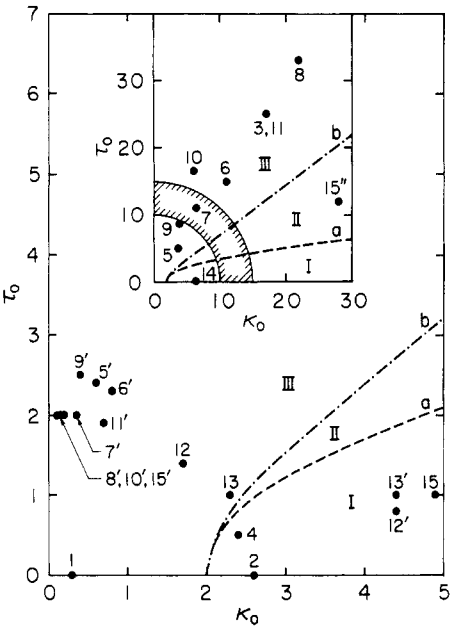

Figure 10. Values of the model parameters plotted in a (κ_0,τ_0) plane. The plane is divided into three domains, I, II, and III, by the broken (a) and chain (b) curves, and the oscillations of $\bar{g}_1^{ij'}$ as functions of t become remarkable for large $\nu = (\kappa_0^2 + \tau_0^2)^{1/2}$ beyond the shaded domain of the insert (see the text). The numbered points are identified with (1) PM, (2) PDMS, (3) POM, (4) POE, (5) i-PP, (5′) s-PP, (6) i-PS, (6′) s-PS, (7) i-PMA, (7′) s-PMA, (8) i-PMVK, (8′) s-PMVK, (9) i-PVAc, (9′) s-PVAc, (10) i-PVC, (10′) s-PVC, (11) i-PVB, (11′) s-PVB, (12) i-PMMA, (12′) s-PMMA, (13) i-PαMS, (13′) s-PαMS, (14) PDLA, (15) amylose in dimethyl sulfoxide, (15′) amylose in aqueous solution in case 2, and (15″) amylose in aqueous solution in case 1.

In the dynamics of the discrete HW chain, it is necessary to evaluate the mean reciprocal (end-to-end) distance $\langle R^{-1}(t)\rangle$ for chains of contour length t. Although the simple analytical expressions for $\langle R^2\rangle$, $\langle S^2\rangle$, $\mathbf{A}$, and $\bar{g}_1^{ij'}$ have been given, the evaluation of $\langle R^{-1}\rangle$ is very laborious. Very recently, a useful interpolation formula for it as a function of t, κ_0, and τ_0 has been constructed to be valid in the domain of $0 < \nu < 8$ and $(\kappa_0 - 8)^2 + \tau_0^2 \gtrsim 4$ and in the domain III for $\nu \gtrsim 20$ of Figure 10.[9] Thus, this formula applies to the polymers listed in Table I except i-PMA ($\kappa_0 = 6.5$, $|\tau_0| = 11$) and i-PVAc ($\kappa_0 = 4.0$, $|\tau_0| = 8.6$). Therefore, an interpolation formula for these two polymers has been constructed here following the procedure of ref 9. Then,

$\langle R^{-1} \rangle$ for them is given by eq A1 with eq A2–A4 of ref 9, where A_1 in eq A4 of ref 9 is given by eq A5 of ref 9 and the values of A_k (k = 2–7) are given in Table II.

References and Notes

(1) Yamakawa, H. *Macromolecules* **1977**, *10*, 692.
(2) Yamakawa, H.; Fujii, M. *J. Chem. Phys.* **1976**, *64*, 5222; and succeeding papers. These papers are referred to as SMHWC-I, SMHWC-II, and so on.
(3) Yamakawa, H.; Yoshizaki, T. *Macromolecules* **1982**, *15*, 1444.
(4) Flory, P. J. "Statistical Mechanics of Chain Molecules"; Interscience: New York, 1969.
(5) Yamakawa, H.; Yoshizaki, T.; Fujii, M. *Macromolecules* **1977**, *10*, 934; and succeeding papers.
(6) See also: Yamakawa, H.; Fujii, M. *Macromolecules* **1973**, *6*, 407; **1974**, *7*, 128.
(7) Yamakawa, H.; Yoshizaki, T. *J. Chem. Phys.* **1981**, *75*, 1016.
(8) Yamakawa, H.; Yoshizaki, T.; Shimada, J. *J. Chem. Phys.* **1983**, *78*, 560.
(9) Yamakawa, H.; Yoshizaki, T. *J. Chem. Phys.* **1983**, *78*, 572.
(10) Yamakawa, H.; Shimada, J. *J. Chem. Phys.* **1978**, *68*, 4722.
(11) Yamakawa, H.; Shimada, J. *J. Chem. Phys.* **1979**, *70*, 609.
(12) Flory, P. J. *Proc. Natl. Acad. Sci. U.S.A.* **1973**, *70*, 1819.
(13) Yamakawa, H.; Fujii, M. *J. Chem. Phys.* **1977**, *66*, 2584.
(14) Yamakawa, H.; Fujii, M.; Shimada, J. *J. Chem. Phys.* **1976**, *65*, 2371.
(15) Yamakawa, H.; Shimada, J.; Nagasaka, K. *J. Chem. Phys.* **1979**, *71*, 3573. There is a typographical error in eq A17: The asterisk on G in the second line should be deleted.
(16) Kratky, O.; Porod, G. *Recl. Trav. Chim. Pays-Bas* **1949**, *68*, 1106.
(17) Benoit, H.; Doty, P. *J. Phys. Chem.* **1953**, *57*, 958.
(18) Uchida, T.; Kurita, Y.; Koizumi, N.; Kubo, M. *J. Polym. Sci.* **1956**, *21*, 313.
(19) Marchal, J.; Benoit, H. *J. Polym. Sci.* **1957**, *23*, 223.
(20) Bak, K.; Elefante, G.; Mark, J. E. *J. Phys. Chem.* **1967**, *71*, 4007.
(21) Kotera, A.; Suzuki, K.; Matsumura, K.; Nakano, T.; Oyama, T.; Kambayashi, U. *Bull. Chem. Soc. Jpn.* **1962**, *35*, 797.
(22) Mark, J. E.; Flory, P. J. *J. Am. Chem. Soc.* **1965**, *87*, 1415.
(23) Flory, P. J.; Sundararajan, P. R.; DeBolt, L. C. *J. Am. Chem. Soc.* **1974**, *96*, 5015.
(24) Flory, P. J. *Macromolecules* **1974**, *7*, 381.
(25) Ojalvo, E. A.; Saiz, E.; Masegosa, R. M.; Hernández-Fuentes, I. *Macromolecules* **1979**, *12*, 865.
(26) Yoon, D. Y.; Flory, P. J. *J. Polym. Sci., Polym. Phys. Ed.* **1976**, *14*, 1425.
(27) Suter, U. W. *J. Am. Chem. Soc.* **1979**, *101*, 6481.
(28) Sundararajan, P. R. *Macromolecules* **1978**, *11*, 256.
(29) Mark, J. E. *J. Chem. Phys.* **1972**, *56*, 451.
(30) Saiz, E.; Riande E.; Delgado, M. P.; Barrales-Rienda, J. M. *Macromolecules* **1982**, *15*, 1152.
(31) Sundararajan, P. R. *Macromolecules* **1977**, *10*, 623.
(32) Fujii, M.; Nagasaka, K.; Shimada, J.; Yamakawa, H. *J. Chem. Phys.* **1982**, *77*, 986.
(33) Yamakawa, H.; Yoshizaki, T. *Macromolecules* **1980**, *13*, 633.
(34) Jordan, R. C.; Brant, D. A.; Cesàro, A. *Biopolymers* **1978**, *17*, 2617.
(35) Brant, D. A.; Dimpfl, W. L. *Macromolecules* **1970**, *3*, 655.
(36) Everett, W. W.; Foster, J. F. *J. Am. Chem. Soc.* **1959**, *81*, 3459, 3464.
(37) Cowie, J. M. G. *Makromol. Chem.* **1960**, *42*, 230.
(38) Burchard, W. *Makromol. Chem.* **1963**, *64*, 110.
(39) Fujii, M.; Honda, K.; Fujita, H. *Biopolymers* **1973**, *12*, 1177.
(40) Williams, A. D.; Flory, P. J. *J. Polym. Sci., Part A-2* **1968**, *6*, 1945.
(41) Tonelli, A. E. *Macromolecules* **1972**, *5*, 558.
(42) Erman, B.; Marvin, D. C.; Irvine, P. A.; Flory, P. J. *Macromolecules* **1982**, *15*, 664.
(43) Yamakawa, H.; Fujii, M.; Shimada, J. *J. Chem. Phys.* **1979**, *71*, 1611.
(44) Tonelli, A. E. *Macromolecules* **1973**, *6*, 503.
(45) Berry, G. C.; Nomura, H.; Mayhan, K. G. *J. Polym. Sci., Part A-2* **1967**, *5*, 1.
(46) Barrales-Rienda, J. M.; Pepper, D. C. *J. Polym. Sci., Part B* **1966**, *4*, 939; *Eur. Polym. J.* **1967**, *3*, 535.
(47) Akers, P. J.; Allen, G.; Bethell, M. J. *Polymer* **1968**, *9*, 575.
(48) Shultz, A. R. *J. Polym. Sci., Part A-2* **1970**, *8*, 883.
(49) Troxell, T. C.; Scheraga, H. A. *Macromolecules* **1971**, *4*, 528.
(50) Shmueli, U.; Traub, W.; Rosenheck, K. *J. Polym. Sci., Part A-2* **1969**, *7*, 515.
(51) Yamakawa, H.; Shimada, J.; Fujii, M. *J. Chem. Phys.* **1978**, *68*, 2140.
(52) Yoon, D. Y.; Flory, P. J. *Polymer* **1975**, *16*, 645.
(53) Stockmayer, W. H.; Jones, A. A.; Treadwell, T. L. *Macromolecules* **1977**, *10*, 762.
(54) Fawcett, A. H.; Heatley, F.; Ivin, K. J.; Stewart, C. D.; Watt, P. *Macromolecules* **1977**, *10*, 765.
(55) Matsuo, K.; Stockmayer, W. H.; Mashimo, S. *Macromolecules* **1982**, *15*, 606.

Expansion of Perturbed Rotational Isomeric State Polymethylene Stars

Wayne L. Mattice

Department of Chemistry, Louisiana State University, Baton Rouge, Louisiana 70803.

Received December 28, 1982

ABSTRACT: Expansion is considered for finite, regular polymethylene stars perturbed by the excluded volume effect. A rotational isomeric state model is used for the chain statistics. The number of bonds in each branch ranges up to 10 240, and the functionality of the branch point ranges up to 20. The form of the calculation employed here provides a lower bound for the expansion. If the number, n, of bonds in the polymers is held constant, expansion is found to decrease with increasing branch point functionality. Two factors dictate the manner in which finite stars approach the limiting behavior expected for very large stars. These two factors are the chain length dependence at small n of the characteristic ratio and of $(\alpha^5 - \alpha^3)/n^{1/2}$. In very good solvents these two factors reinforce one another, but they tend to cancel in solvents in which polymer expansion is small.

Rotational isomeric state theory permits construction of realistic models for polymer chains.[1] These models incorporate expected values for bond lengths, angles between bonds, and short-range contributions to energy barriers to rotation about bonds. Matrix methods provide the formalism required for rigorous evaluation of statistical mechanical averages of configuration-dependent physical properties for the unperturbed chain. Generator matrix calculations require negligible computer time even in the case of long chains. The theorem on direct products permits rigorous extension to branched polymers.[2-4] Unperturbed tri- and tetrafunctional polymethylene stars

0024-9297/83/2216-1623$01.50/0